EQUINE VETERINARY JOURNAL
Equine vet. J. (2003) **35** (7) 00-00

Ultrasonography of the equine cervical region: a descriptive study in eight horses

L. C. BERG, J. V. NIELSEN, M. B. THOEFNER† and **P. D. THOMSEN***

Departments of Anatomy and Physiology and †*Large Animal Surgery, The Royal Veterinary and Agricultural University of Copenhagen, Bülowsvej 17, DK-1870 Frederiksberg C, Denmark.*

Keywords: horse; neck; ultrasonography; anatomy; articular facet

Summary

Reasons for performing study: **In equine patients, the cause of clinical signs possibly related to the cervical region is often difficult to diagnose. Ultrasonography allows quick and noninvasive visualisation, but reference material of the normal equine neck is needed.**

Objectives: **To describe and document the normal ultrasonographic appearance of transverse scans in the cervical region with emphasis on the synovial articular facet joints, cervical vertebrae and paravertebral structures; and further, to provide images of frozen cross-sections for anatomical reference.**

Methods: **A study describing the normal ultrasonographic appearance of the cervical anatomy was performed. Transverse scans were obtained from second cervical vertebra (C2) to first thoracic vertebra (T1).** ***Post mortem*** **photographs of frozen cross-sections were obtained as anatomical reference.**

Results: **The structures were clearly visualised by ultrasonography and consistency was found between ultrasonographic images and corresponding cross-sectional anatomy. The articular facets varied between horses and facets (C2 to T1). Discrepancy in the existing anatomical descriptions was found.**

Conclusions and potential relevance: **The anatomical and ultrasonographic description provides a reference for ultrasonographic evaluation of equine cervical facet joints, vertebrae and paravertebral structures. The findings and variations found are considered to reflect the naturally occurring variations in horses.**

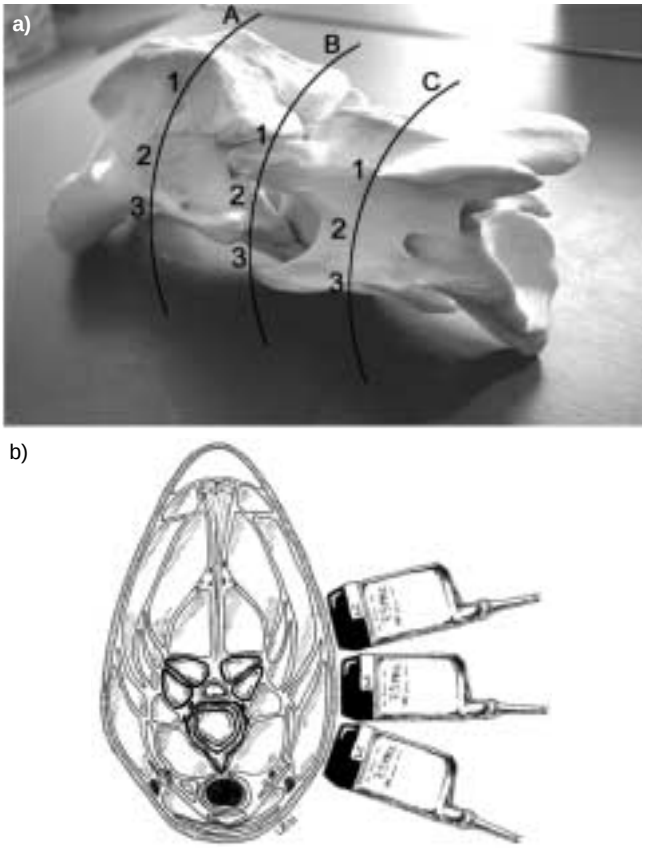

Fig 1: Position of the transducer in relation to the vertebrae. a) The transducer position for mid-vertebral images of the axis (A), images at the level of the widest point of the facet (B) and images at the level of the mid-vertebrae (C) are shown in dorsal (1), middle (2) and ventral views (3). b) The transducer positions are shown on a transverse image of the facet.

Introduction

Diagnosis of an equine patient with clinical signs possibly related to the cervical region is difficult. Radiography is a useful and well-documented diagnostic technique that offers the possibility of evaluating superficial and profound bony changes and visualising the vertebral canal. However, in general practice, difficulties have been described in obtaining diagnostic images of more specific sites of interest (Hager 1986; Craychee 1998).

Ultrasonography is a relatively recent diagnostic technique which offers a quick and noninvasive visualisation of soft tissue changes such as foreign bodies, atrophy and fibrosis of muscles (Hager 1986; Craychee 1998), as well as evaluation of the outline of bone and joints (Harcke *et al.* 1988). Furthermore, Nazarian *et al.* (1998) have described the evaluation of articular facets, nerve roots and paraspinal tissue in human subjects using ultrasound. Compared to radiography, ultrasonography is a dynamic diagnostic modality. A simple static ultrasonographic picture may

*Author to whom correspondence should be addressed.
[Paper received for publication 12.08.02; Accepted 13.12.02]

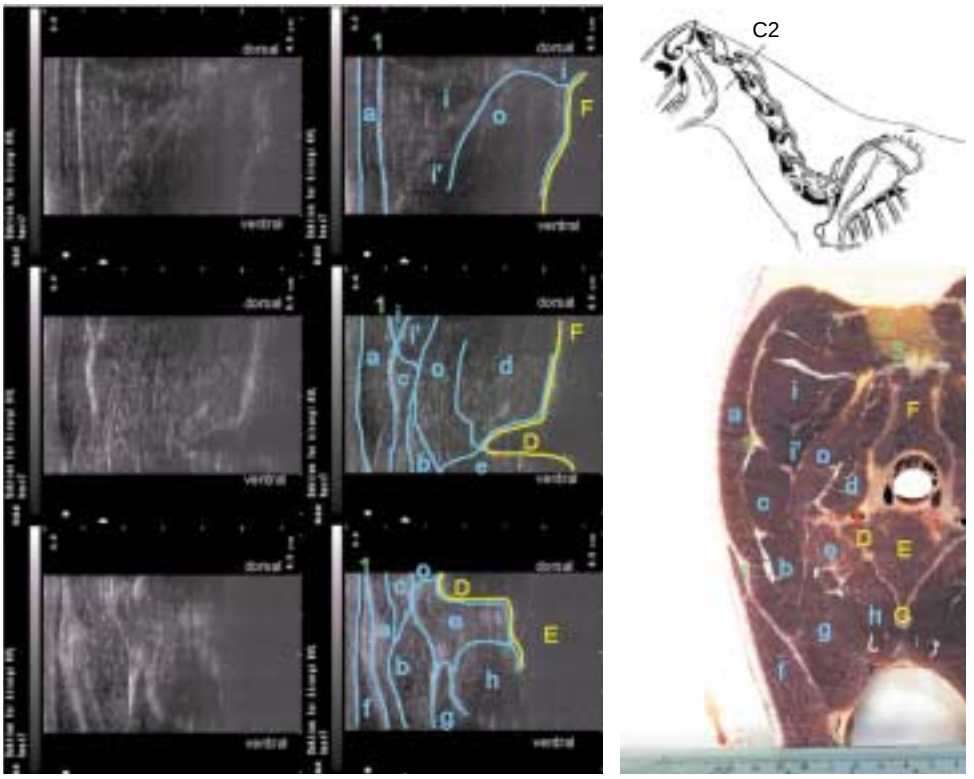

Fig 2: Identifiable structures on ultrasound images and anatomical cross-section at the level of C2. Muscles: M. splenius *(a);* m. longissimus atlantis *(b);* m. longissimus capitis *(c);* mm. multifidii cervicii *(d);* mm. intertransversarii cervicii *(e);* m. brachiocephalicus *(f);* m. longus capitis *(g);* m. longus colli *(h);* m. semispinalis capitis (i/i')*;* m. obliquus capitis caudalis *(o). Vertebral:* Processus transversus *(D);* corpus vertebra *(E);* processus spinosus *(F);* crista ventralis *(G). Misc.:* Fascia cervicalis *(1);* funiculus nuchae *(2);* laminae nuchae *(3);* a. et v. vertebralis (x).

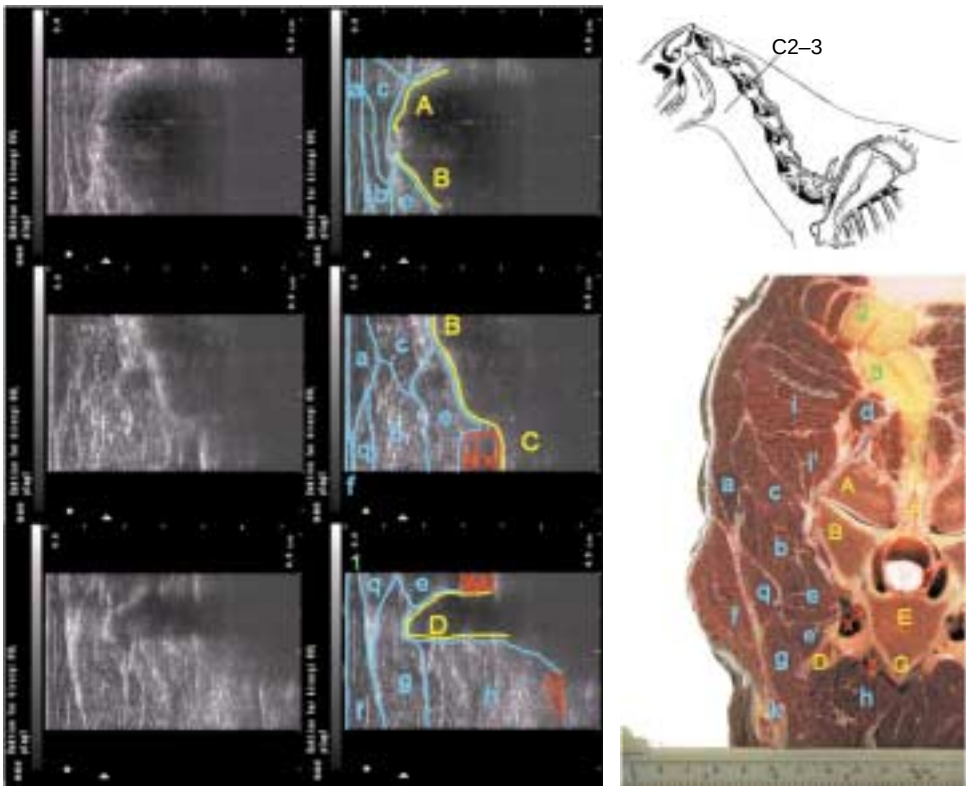

Fig 3: Identifiable structures on ultrasound images and anatomical cross-section at the level of C2–C3. Muscles: M. splenius *(a);* m. longissimus atlantis *(b);* m. longissimus capitis *(c);* mm. multifidii cervicii *(d);* mm. intertransversarii cervicii *(e);* m. intertransversarius ventralis cervicis (e')*;* m. brachiocephalicus *(f);* m. longus capitis *(g);* m. longus colli *(h);* m. semispinalis capitis (i/i')*;* m. omohyoideus *(k);* m. omotransversarius *(q). Vertebral:* Processus articularis caudalis *(A);* processus articularis cranialis *(B);* processus transversus *(D);* corpus vertebra *(E);* processus spinosus *(F);* crista ventralis *(G). Misc.*: Fascia cervicalis *(1);* laminae nuchae *(2);* funiculus nuchae *(3);* a. et v. vertebralis *(x); rami from vertebral vessels (y).*

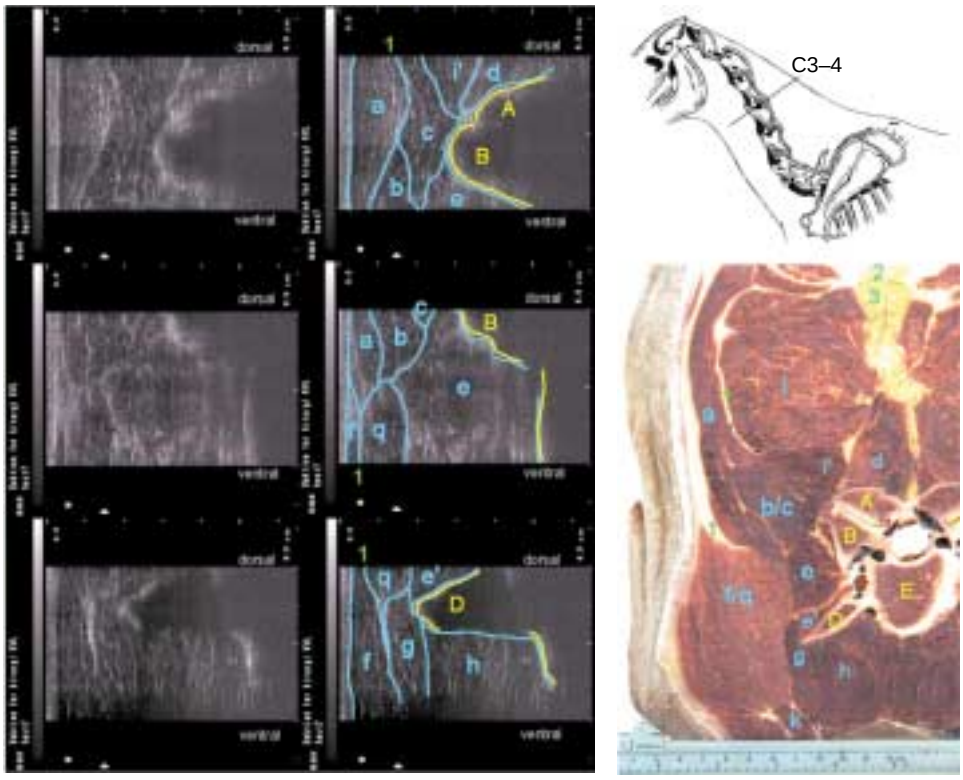

Fig 4: Identifiable structures on ultrasound images and anatomical cross-section at the level of C3–C4. Muscles: M. splenius *(a);* m. longissimus atlantis *(b);* m. longissimus capitis *(c);* mm. multifidii cervicii *(d);* mm. intertransversarii cervicii *(e);* m. brachiocephalicus *(f);* m. longus capitis *(g);* m. longus colli *(h);* m. semispinalis capitis (i/i'); m. obliquus capitis caudalis *(o). Vertebral:* Processus transversus *(D);* corpus vertebra *(E);* processus spinosus *(F);* crista ventralis *(G). Misc.:* Fascia cervicalis *(1);* funiculus nuchae *(2);* laminae nuchae *(3);* a. et v. vertebralis (x).

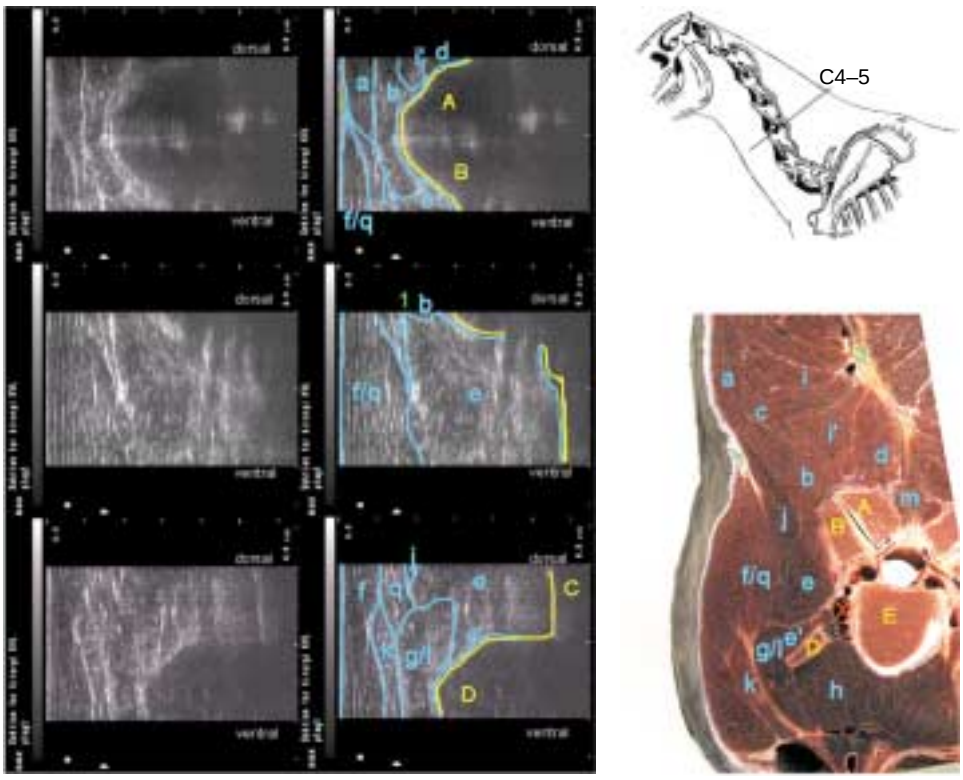

Fig 5: Identifiable structures on ultrasound images and anatomical cross-section at the level of C4–C5. Muscles: M. splenius *(a);* m. longissimus atlantis *(b);* m. longissimus capitis *(c);* mm. multifidii cervicii *(d);* mm. intertransversarii cervicii *(e);* m. brachiocephalicus *(f);* m. longus capitis *(g);* m. longus colli *(h);* m. semispinalis capitis (i/i'); m. obliquus capitis caudalis *(o). Vertebral:* Processus transversus *(D);* corpus vertebra *(E);* processus spinosus *(F);* crista ventralis *(G). Misc.:* Fascia cervicalis *(1);* funiculus nuchae *(2);* laminae nuchae *(3);* a. et v. vertebralis (x).

not reveal the same amount of information as a radiograph However, with ultrasound it is possible to perform assessments of structures in motion, whereby additional information is obtainable. The potential of dynamic imaging has been demonstrated in local application of pharmaca (Küllmer *et al.* 1997) and in surgical treatment of various conditions such as drainage of muscular abscesses or haematomas and removal of foreign bodies (Hager 1986; Craychee 1998). The potential for operator-induced artefacts and the subjective interpretation of images should always be considered. Therefore, a detailed knowledge of the cross-sectional anatomy is a prerequisite for good results.

To our knowledge, no report on ultrasonography of the normal equine neck exists in the literature. The objective of this study was to describe and document the normal ultrasonographic appearance of transverse scans in the cervical region with an emphasis on the synovial articular facet joints, cervical vertebrae and paravertebral structures.

Materials and methods

Horses

Eight horses with unknown clinical history, purchased for anatomical educational purposes, were subjected to a systematic clinical and radiological examination and were included only if no pathological changes were found in the cervical region. Their mean height was 138 cm at the withers (range 125–155 cm), which is low compared to standard riding horses; and mean age was 7.75 years, evaluated from the teeth (range 2.5–14 years). Four horses were in normal body condition, 3 below average and one above average. The clinical examination consisted of vital parameter assessment, lameness examination and a basic neurological examination. The lameness examination included walking and trotting in a straight line on a hard surface, and walking, trotting and cantering on the lunge on a soft surface. Flexion tests were performed on all 4 limbs. If lameness was present, local analgesia was used to establish whether the pain originated from the leg. Signs of ataxia/proprioceptive dysfunction or weakness were assessed by turning the horse in tight circles and performing the ‘sway’ and ‘tail-pull’ tests when standing and at the walk. The neck was palpated and evaluated for signs of asymmetry or skeletal abnormality and manipulated dorsoventrally and laterally to evaluate range of movement (Rose and Hodgson 1993; Hahn *et al.* 1999). Finally, cervical radiographs were obtained using a laterolateral projection with the horses in a standing position and the cervical vertebrae numbered during exposure. The cervical vertebrae were evaluated for changes in size and outline.

Preparation and equipment

The B&K Medical Ultrasound System 3535[1] was used with a 7.5 MHz straight linear array transducer. No stand-off was used. Prior to the ultrasonographic examination, optimal settings for gain, resolution and frame rate were determined. A horse of medium size and weight was used and images repeated at different settings to determine the optimum values. The final values for the study were 30% gain, a resolution of 6 and a frame rate of 39 frames/sec. For optimal transducer contact, the necks of the horses were shaved, washed and a scanning gel applied. The horses were positioned in a restraining stall with the forelimbs next to each other and with the neck in a relaxed degree of flexion. The facet joints on the left side were located by palpation and/or ultrasonography, and images of the structures at the level of the facet joints and mid-vertebrae recorded. Some horses had to be mildly sedated for this part of the study due to the large amount of scans performed. The images were recorded using a series of 3 images/area starting dorsally at the widest point of the articular facet or the lowest point of the *arcus vertebra* and moving ventrally (Fig 1). The transducer was held transverse to the line of the vertebrae (Fig 1) with the screen showing ventral to the left. The focus was at 1.5 cm from C2–C7 and at 3 cm at C7–T1.

Image evaluation

Following the storage of ultrasound images on floppy disks in TIFF format, the horses were subjected to euthanasia and the necks separated from the rest of the bodies and frozen. Once frozen, the necks were sliced by bandsaw into cross-sections at the widest points of the articular facets and at the middle of the vertebrae to be comparable with the ultrasonographic images. All frozen cross-sections were photographed. When defrosted, the cross-sections were thoroughly dissected, exposing the bony surfaces to assess normality further. The ultrasonographic and cross-sectional images were studied and structures identified. The structures found in the ultrasonographic images were compared across the 8 horses for consistency in appearance and further compared with the anatomy of the prepared cross-sections, with clean bones of the cervical vertebral columns and with the existing literature.

Results

The normal anatomy is depicted in a series of transverse images starting at the second cervical vertebra (C2) and continuing to the articulation of C7–T1 (Figs 2–9). In all ultrasonographic images, the cutaneous and subcutaneous layers appeared as a hyperechoic zone enclosed by more hyperechoic lines. A hypoechoic area between the cutis/subcutis and the muscle tissue consistent with fat tissue is apparent in Figure 4. The thickness of the cutaneous and subcutaneous layer varied depending on the condition of the horse and the amount of transducer pressure exerted while obtaining the image.

Vertebrae

The ultrasonographic outlines of the vertebrae were visible with hyperechoic borders followed by shadowing due to strong reflection from the osseous tissue. There was good consistency between the ultrasonographic images and the cross-sections at the location of the articular facets (Figs 3, 4, 5, 7, 8 and 9[A,B]). The size, shape and outline of the cranial and caudal articular processes showed a high degree of variation between images of the same facet in different horses and also between different facets in the same horse. The irregularity of the articular processes, seen in scans, was consistent with the cross-sections and the clean bones. No clear distinction of the articular cartilage was possible on any of the ultrasonographic images. The ventral tuberculum of the transverse process was visible ventrally in all

ultrasonographic images of the facet, although it was inconsistently visible in the cross-section anatomical preparations. In these cases, the process was always palpable within a few millimetres of the section. At the mid-vertebral level there was good agreement between the ultrasonographic images and frozen cross-sections (Figs 2 and 6). The vertebral arch and the area narrowing towards the rudimentary spinous process were clearly visible, although without the process itself being visible. The transverse process was visible ventrally and the slope towards the ventral crest was apparent ventral to the transverse process, again without the crest itself being visible. The differing outline of the mid-axis (C2) compared to C3–C7 was apparent with its prominent spinous process and ventral crest and smaller transverse processes (Fig 2[D,F,G]).

The joint space was easily identified in all images, although the extent of the visible joint space varied between different facet joints in the same horse and between the same joints in different horses (Figs 3, 4, 5, 7, 8 and 9). This was different from the frozen cross-sections, which showed an almost constant joint space. A frequent finding in the case of a wide joint space was a homogenous echoic area not consistent with anechoic synovial fluid (Fig 7). When dissection was carried out, intra-articular synovial folds of varying size were present in 94% of all articular facet joints. Histology of these folds showed the presence of synoviocytes and adipose cells (Fig 10) (H.E. Jensen, personal communication).

On the lateral surface of the vertebrae between the articular facet and the transverse process and medial to the *intertransversarii* were vague hypoechoic structures with hyperechoic borders, consistent with the large vessels *a. et v. vertebralis* (Fig 3[x]) and their rami (Figs 3 and 9[y]).

Muscles

The muscle tissue had a heterogeneous appearance. The large muscle layers could be distinguished and identified, with the hyperechoic collageneous tissue of the *fascia cervicalis* outlining many of the muscular structures (Figs 2, 3, 4, 6, 7, 8 and 9[1]). In a few images, muscles were seen as separate structures in the ultrasonographic images, which could not be differentiated on the anatomical cross-sections (Figs 4 and 5). The distinguishable epaxial extensor muscles were the *m. longissimus atlantis* (Figs 2–8[b]) and the *m. longissimus capitis* (Figs 2–4[c]) lateral to the facet and, in the caudal part of the neck, *m. longissimus cervicis* (Figs 8–10[n]). Their individual outlines were visible in only some images but they all passed over the tip of the facet joint with the *atlantis* lateroventral to the *capitis*. The *cervicis* first appeared at the level of C6, ventral to the other two. Parts of the transversospinalis system were also visible; *mm. multifidii cervicii* dorsal to the facets with origins on the articular processes (Figs 2–9[d]), *m. semispinalis capitis*, which were divided into 2 dorsal to the longissimus group (Figs 2–6[i,i']) and *m. obliquus capitis caudalis* (Fig 2[o]) dorsal to the axis. *Mm. intertransversarii cervicii dorsalis* (Figs 2–9[e]) *et ventralis* (Figs 3–5[e']) were easily identified as a muscular structure between the articular facets and the transverse processes with *pars ventralis* in close proximity to the transverse process, although this was clearly distinguishable in only a few images. *M. semispinalis capitis*, *mm. intertransversarii cervicii dorsalis et ventralis* and *mm. multifidii cervicii* had a high content of tendinous strips difficult to differentiate from fascia, rendering their outline more difficult to distinguish in Figures 2–9. The identifiable hypaxial flexor muscles *mm. longus colli* (Figs 2–9[h]) *et capitis* (Figs 2–5[g]) were visible around and ventral to the transverse processes with *m. longus colli* placed more medial. *M. longus capitis* spanned only from C1 to C4. They had a common fascia, *laminae praevertebralis*, causing them to appear as one structure in some images in both scans and cross-sectional anatomy (Fig 5).

In the superficial muscle layers, *m. splenius* (Figs 2–9[a]) were the more lateral from C2 to C4, after which *m. serratus ventralis* (Figs 5–9[j]) appeared on the lateral surface. *M. brachiocephalicus* (Figs 2–9[f]) and *m. omotransversarius* (Figs 3–9[q]) were closely related, with the brachiocephalic muscle slightly ventrolaterally. They were visible as a group ventrolaterally in both scans and cross-sections. Ventral to the transverse processes, *m. omohyoideus* (Figs 5–8[k]) and *m. scalenus ventralis* (Figs 5–9[l]) *et medius* (Figs 8–9[l']) were found as a muscular structure without clear individual separation in the ultrasonographic images. Furthermore, in ultrasound images, *m. scalenus ventralis* was inseparable from *m. longus capitis* (Fig 5). In none of the ultrasonographic images was *m. cutaneus colli* identified, but it was visible in some of the anatomical preparations (Figs 4?6). The muscular structures were generally divided by fascial sheets but, with the longissimus group, the brachiocephalic omotransversarius and the ventrolateral group (comprising *m. longus colli et capitis*, *m. omohyoideus* and *mm. scalenus ventralis et medius*) were difficult to differentiate individually on both ultrasonographic images and cross-sections (Figs 2–9). As in the subcutaneous layer, the thickness of the individual muscles varied with transducer pressure exerted by the operator.

Discussion

The detailed anatomy of the equine neck has received little attention. The literature on the subject is limited and almost exclusively shows the area in a lateral projection. To produce reliable interpretation during ultrasonography, a thorough knowledge of both transverse and longitudinal anatomy is required. In the present study, the anatomy of frozen cross-sections was compared to images obtained by transverse ultrasonographic scans. Good agreement between the ultrasonographic images and corresponding cross-sections was found. Minor variations were attributable to the angle of the transducer, pressure exerted by the operator and the position of the neck of the horse. This is particularly evident in the evaluation of thickness of individual muscles and position of the articular processes in relation to each other.

The cervical articular facet joints are larger than the facet joints of other regions of the horse (Nickel *et al.* 1986; Schaller 1992). The joint space and articular processes can be localised and their outline followed without difficulty. A large variation in the outline of the irregular articular facet, both on the ultrasonographic images and in the anatomical preparations, was found. This irregularity was caused by the insertions of the epaxial muscles, which were in agreement with Nickel *et al.* (1986) and Schaller (1992) and the uneven bony surfaces of the articular processes themselves (Nickel *et al.* 1986). In the clinical situation, the uneven structure and irregular shape of the articular facet means that minor osteophytosis and enlargements are difficult to identify using ultrasonography. This problem is

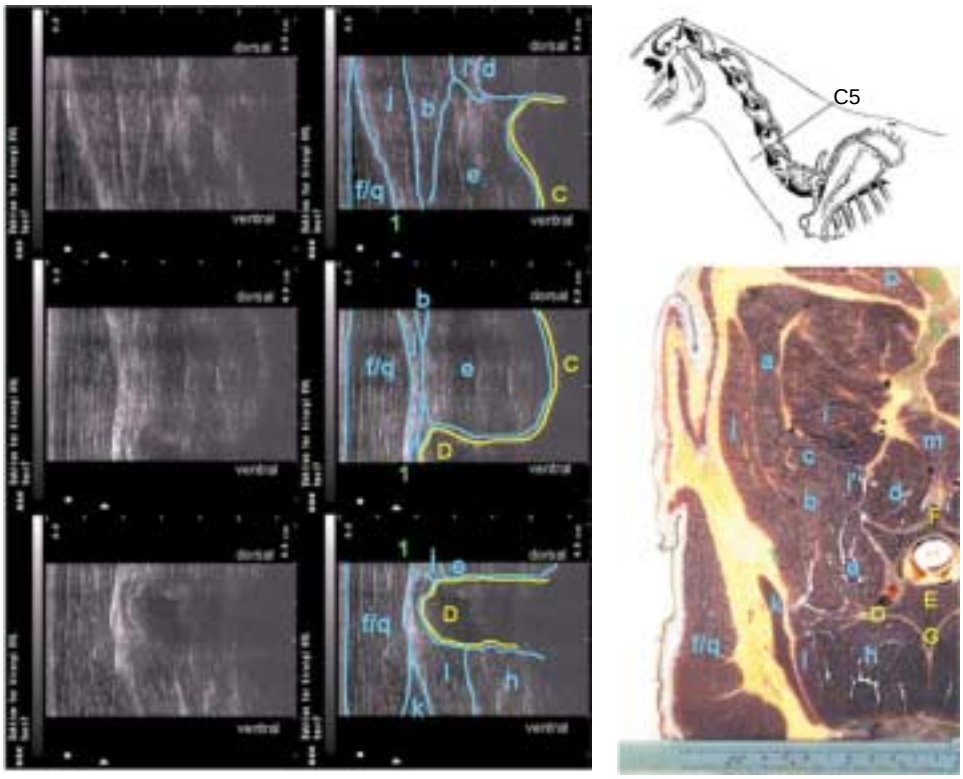

Fig 6: Identifiable structures on ultrasound images and anatomical cross-section at the level of C5. Muscles: M. splenius *(a);* m. longissimus atlantis *(b);* m. longissimus capitis *(c);* mm. multifidii cervicii *(d);* mm. intertransversarii cervicii *(e);* m. brachiocephalicus *(f);* m. longus capitis *(g);* m. longus colli *(h);* m. semispinalis capitis (i/i')*;* m. obliquus capitis caudalis *(o). Vertebral:* Processus transversus *(D);* corpus vertebra *(E);* processus spinosus *(F);* crista ventralis *(G). Misc.:* Fascia cervicalis *(1);* funiculus nuchae *(2);* laminae nuchae *(3);* a. et v. vertebralis (x).

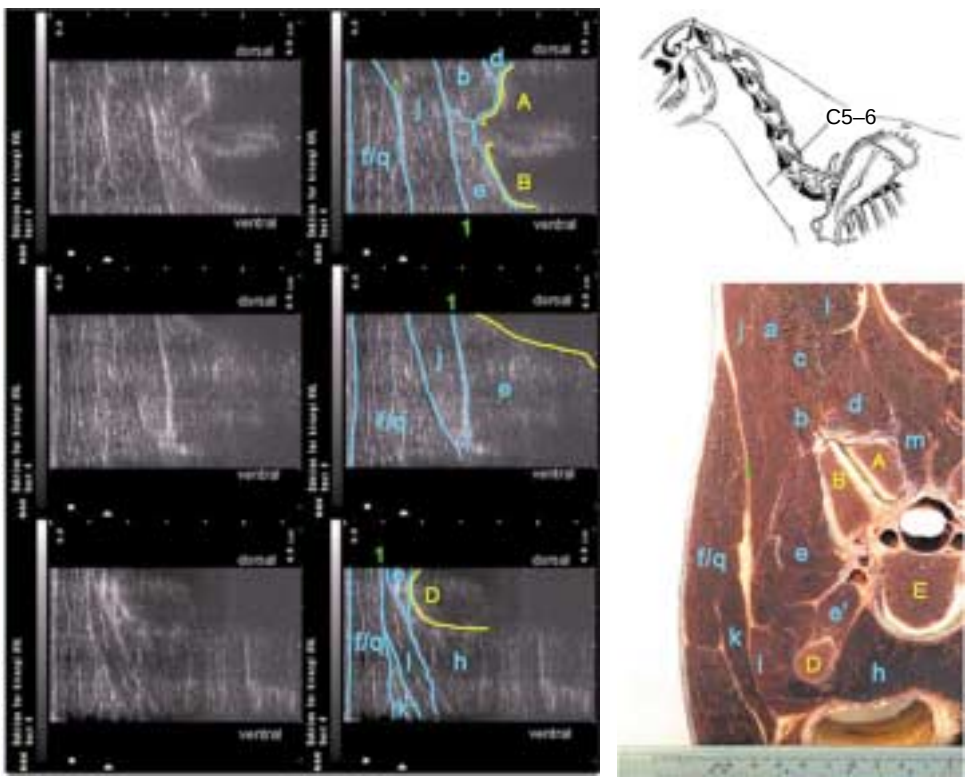

Fig 7: Identifiable structures on ultrasound images and anatomical cross-section at the level of C5–C6. Muscles: M. splenius *(a);* m. longissimus atlantis *(b);* m. longissimus capitis *(c);* mm. multifidii cervicii *(d);* mm. intertransversarii cervicii *(e);* m. brachiocephalicus *(f);* m. longus capitis *(g);* m. longus colli *(h);* m. semispinalis capitis (i/i')*;* m. obliquus capitis caudalis *(o). Vertebral:* Processus transversus *(D);* corpus vertebra *(E);* processus spinosus *(F);* crista ventralis *(G). Misc.:* Fascia cervicalis *(1);* funiculus nuchae *(2);* laminae nuchae *(3);* a. et v. vertebralis (x).

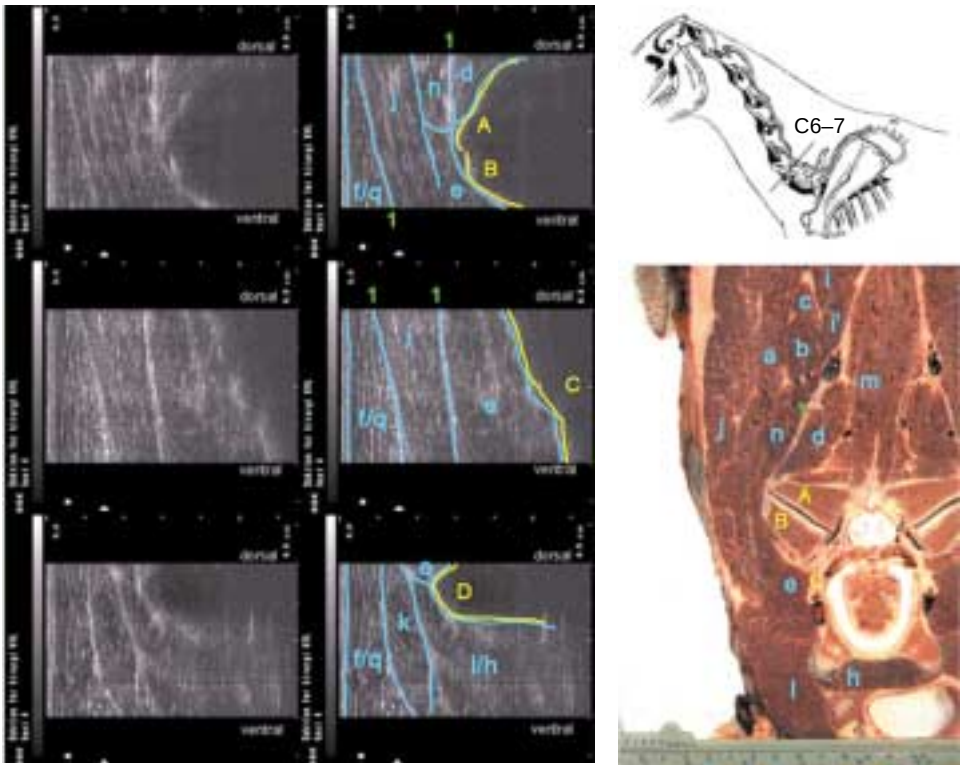

Fig 8: Identifiable structures on ultrasound images and anatomical cross-section at the level of C6–C7. Muscles: M. splenius *(a);* m. longissimus atlantis *(b);* m. longissimus capitis *(c);* mm. multifidii cervicii *(d);* mm. intertransversarii cervicii *(e);* m. brachiocephalicus *(f);* m. longus colli *(h);* m. semispinalis capitis *(i/i');* m. serratus ventralis cervicis *(j);* m. omohyoideus *(k);* mm. scaleni *(l);* m. spinalis cervicis *(m);* m. longissimus cervicis *(n);* m. omotransversarius *(q). Vertebral:* Processus articularis caudalis *(A);* processus articularis cranialis *(B);* arcus vertebra *(C);* processus transversus *(D). Misc.:* Fascia cervicalis *(1);* a. et v. vertebralis *(x).*

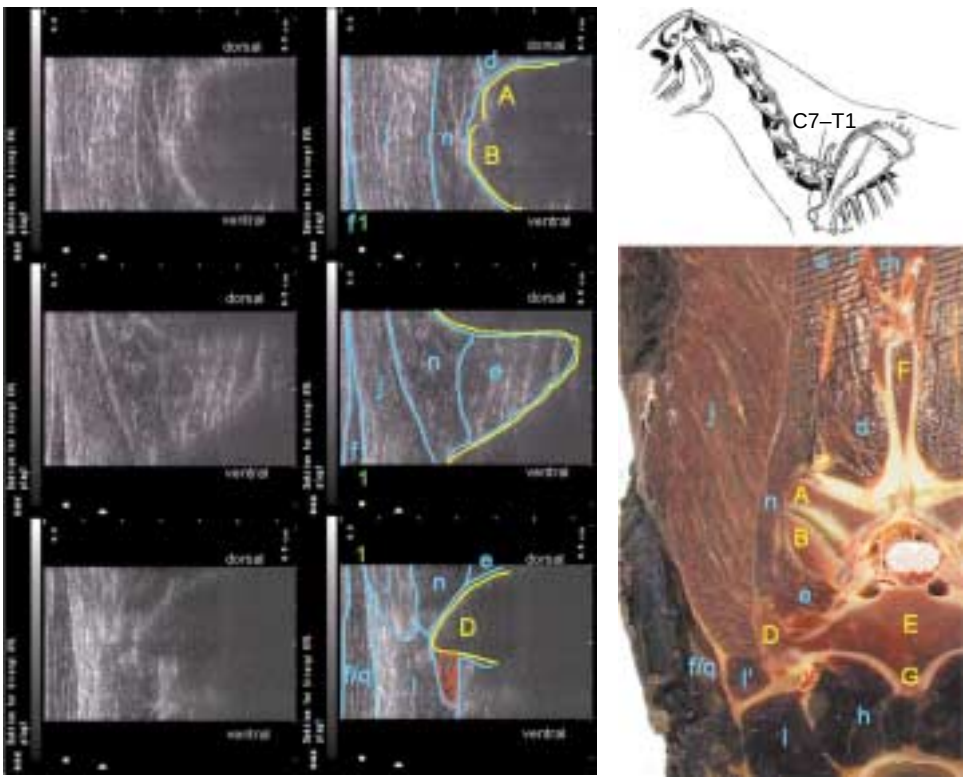

Fig 9: Identifiable structures on ultrasound images and anatomical cross-section at the level of C7–T1. Muscles: M. splenius *(a);* mm. multifidii cervicii *(d);* mm. intertransversarii cervicii *(e);* m. brachiocephalicus *(f);* m. longus colli *(h);* m. semispinalis capitis *(i);* m. serratus ventralis cervicis *(j);* m. scalenus ventralis *(l);* m. scalenus medius *(l');* m. spinalis cervicis *(m);* m. longissimus cervicis *(n);* m. omotransversarius *(q). Vertebral:* Processus articularis caudalis *(A);* processus articularis cranialis *(B);* processus transversus *(D);* corpus vertebra *(E);* processus spinosus *(F);* crista ventralis *(G). Misc.:* Fascia cervicalis *(1); rami from vertebral vessels (y).*

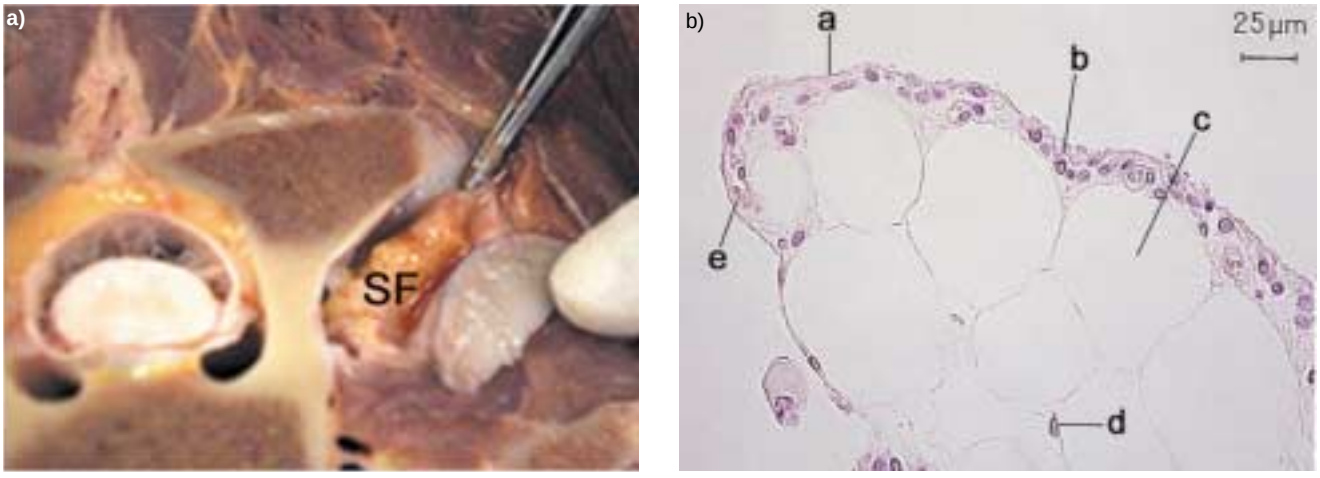

*Fig 10: a) Macroscopic and b) microscopic synovial fold. a) A synovial fold (SF) is visible between the articular processes of the facet joint. b) In the histological preparation of the fold the synovial membrane (*a*) is visible with presence of synoviocyts (*b*) and capillaries (*e*). There is a high content of adipose tissue (*c*) with easily distinguishable fat cells (*d*).*

similar to those described when radiographs of the same structures are evaluated (Hager 1986; Craychee 1998). Harcke *et al.* (1988) described the appearance of joint cartilage in ultrasonographic images as a hypoechoic zone bordered by an outer hyperechoic line caused by the transition from cartilage to synovial fluid and an inner hyperechoic line caused by the bone. These findings have not been confirmed by this study and would be seen only if a perpendicular projection of the ultrasound beam on the cartilage was created.

The images were obtained at the widest point of the articular facets and most distinct outline of the bony structures, at the cost of some muscular definition. The result is that all the individual muscles are not clearly distinguishable in all the ultrasonographic images. The echogenicity of the muscles is consistent with Reef (1998), in that they have a heterogeneous appearance due to hypoechoic muscle fibres, fat tissue and varying degree of hyperechoic collagenous fibres. Furthermore, there is consistency between the appearance of hyperechoic lines in the ultrasonographic images and the fascia outlining the muscles and tendinous strips permeating *m. semispinalis capitis*, *mm. multifidii cervicii* and *mm. intertransversarii cervicii*. The positions of the identifiable muscles are consistent with Nickel *et al.* (1986) and Schaller (1992) on both ultrasonographic images and anatomical cross-sections. However, some muscles are difficult to differentiate on ultrasonographic images as well as anatomical cross-sections and are therefore not easily identified. This applies especially to the longissimus muscles and the ventral group comprising *mm. scalenus*, *m. omohyoideus*, *m. longus colli et m. longus capitis*. The literature (Ellenberger and Baum 1894; Nickel *et al.* 1986; Ashdown and Done 1987; Schaller 1992; Popesko 1993) does not offer a precise description of the position of these muscles in relation to each other in a transverse projection. *Mm. longissimus atlantis et capitis* both run along the entire length of the neck, but their position lateroventral to *m. semispinalis capitis* on the drawings of Ellenberger and Baum (1894), Nickel *et al.* (1986), Schaller (1992) and Popesko (1993) is difficult to locate on the cross-sectional anatomical preparations and the ultrasonographic images. According to Schaller (1992) *m. semispinalis capitis* has 2 parts (*m. biventer et m. complexus*), whereas Nickel *et al.* (1986) refer to only one part in the horse. This makes defining the extent of the muscle in relation to the longissimus muscles even more complicated. The insertion of *m. scalenus ventralis* is on the transverse processes of C3 to C6 according to Schaller (1992). The lateral figures of Nickel *et al.* (1986) and Popesko (1993) also show the muscle ranging from C3, but in the transverse figures of the literature it does not appear until C6 (Ellenberger and Baum 1894; Nickel *et al.* 1986; Popesko 1993). In the present study, it cannot be seen until C5–6.

The anatomical and ultrasonographical knowledge provided by this study generates the possibility of ultrasonographic evaluation of equine cervical facet joints, vertebrae and paravertebral structures by presenting a description of the region usable as reference. Since dissection of the necks verified the absence of gross pathological changes, the findings and variations found in these 8 horses are considered to reflect the findings and naturally occurring variations in clinically normal horses with no pathological changes. The present study did not include evaluation of cervical nerve roots as described in human medicine (Nazarian *et al.* 1998) but, with impingement of nerve roots being described in equine medicine (Moore *et al.* 1992; Ricardi and Dyson 1993), this provides an interesting perspective.

Acknowledgements

The authors would like to thank Dr Svend Kold for constructive criticism and support, Associate Professor of Radiology Jens Arnbjerg and his staff for assistance during the radiographic examination and Erling Nielsen and the staff of the Section of Anatomy and Cell Biology and Department of Large Animal Surgery for invaluable assistance throughout the study. Professor H.E. Jensen of the Department of Pharmacology and Pathobiology was kind enough to prepare and analyse histological sections of the synovial folds.

Manufacturer's address

[1]B&K Medical, Gentofte, Denmark.

References

Anon (1992) *Nomina Anatomica Veterinaria*, International Committee on Veterinary Anatomical Nomenclature, World Association of Veterinary Anatomists.

Ashdown, R.R. and Done, S.H. (1987) *Color Atlas of Veterinary Anatomy - The Horse*, Vol. 2, Mosby-Wolfe, London.

Craychee, T.J. (1998) Ultrasonographic evaluation of equine musculoskeletal injury. In: *Equine Diagnostic Ultrasonography*, Ed: N.W. Rantanen and A.O. McKinnon, Williams & Wilkins, Baltimore. pp 265-304.

Ellenberger, W. and Baum, H. (1894) *Anatomie des Pferdes II, Kopf und Hals*, 1st edn., Verlag von Paul Parey, Berlin. pp 338-357.

Hager, D.A. (1986) The diagnosis of deep muscle abscesses using two-dimensional real time ultrasound. *Proc. Am. Ass. equine Practnrs.* **??**, 523-529.

Hahn, C.N., Mayhew, I.G. and MacKay, R.J. (1999) Diseases of the nervous system. In: *Equine Medicine and Surgery*, Vol. 1, 5th edn., Eds: P.T. Colahan, A.M. Merritt, J.N. Moore and I.G. Mayhew, Mosby Inc., St. Louis. pp 865-983.

Harcke, H.T., Grissom, L.E. and Finkelstein, M.S. (1988) Evaluation of the musculoskeletal system with sonography. *Am. J. Roentgenol.* **150**, 1253-1261.

Küllmer, K., Rompe, A., Löwe, A., Herbsthofer, B. and Eysel, P. (1997) Die sonographie der lendenwirbelsäule und des lumbosakralen überganges. *Wirbelsäule* **135**, 310-314.

Moore, B.R., Holbrook, T.C., Stefanacci, J.D., Reed, S.M., Tate, L.P. and Menard, M.C. (1992) Contrast-enhanced computed tomography and myelography in six horses with cervical stenotic myelopathy. *Equine vet. J.* **24**, 197-202.

Nazarian, L.N., Zegel, G., Gilbert, K.R., Edell, S.S., Bakst, B.L. and Goldberg, B.B. (1998) Paraspinal ultrasonography: lack of accuracy in evaluating patients with cervical or lumbar back pain. *J. Ultrasound Med.* **17**, 117-122.

Nickel, R., Schummer, A., Seiferle, E., Wilkens, H., Wille, K.H. and Frewein, J. (1986) *The Anatomy of the Domestic Animals - The Locomotor System of the Domestic Mammals*, Vol. 1, Verlag Paul Parey, Berlin. pp 24-28, 291-304, 333-340, 350-352.

Popesko, P. (1993) *Atlas der topographischen Anatomie der Haustiere*, Vol. 1, 4th edn., Ferdinand Enke Verlag, Stuttgart. pp 00-00.

Reef, V.B. (1998) *Equine Diagnostic Ultrasound*, W.B. Saunders Co., Philadelphia.

Ricardi, G. and Dyson, S.D. (1993) Forelimb lameness associated with radiographic abnormalities of the cervical vertebrae. *Equine vet. J.* **25**, 422-426.

Rose, R.J. and Hodgson, D.R. (1993) ???. In: *Manual of Equine Practice*, W.B. Saunders Co., Philadelphia. pp 356-391.

Schaller, O. (1992) *Illustrated Veterinary Anatomical Nomenclature*, Ferdinand Enke Verlag Stuttgart, Stuttgart. pp 40-43, 104-111.